Using Quad-Pol and Single-Pol RADARSAT-2 Data for Monitoring Cold Alpine and Outlet Antarctic Glaciers

Olivier Harant, Emmanuel Le Meur, Gabriel Vasile, Lionel Bombrun, Laurent Ferro-Famil, Michel Gay, Emmanuel Trouvé

▶ To cite this version:

HAL Id: hal-00640859
https://hal.archives-ouvertes.fr/hal-00640859

Submitted on 14 Nov 2011

USING QUAD-POL AND SINGLE-POL RADARSAT-2 DATA FOR MONITORING ALPINE AND OUTLET ANTARCTIC GLACIERS

Olivier Harant[1,3], Emmanuel Le Meur[4], Gabriel Vasile[1], Lionel Bombrun[2], Laurent Ferro-Famil[3], Michel Gay[1], Emmanuel Trouvé[5]

[1] *Grenoble-Image-sPeech-Signal-Automatics Lab*
GIPSA-lab DIS/SIGMAPHY, CNRS
Grenoble INP, 961 rue de la Houille Blanche, BP 46 38402 Grenoble, France
{olivier.harant|gabriel.vasile|michel.gay}@gipsa-lab.grenoble-inp.fr

[2] *Université de Bordeaux, UB1, IPB, ENSEIRB-Matmeca, Laboratoire IMS*
UMR 5218, Groupe Signal et Image, Talence, France
lionel.bombrun@ims-bordeaux.fr

[3] *Institute of Electronics and Telecommunications Rennes*
IETR SAPHIR, CNRS
Université de Rennes 1, Bat. 11D, 263 avenue du Général Leclerc 35042 Rennes, France
Laurent.Ferro-Famil@univ-rennes1.fr

[4] *Laboratoire de glaciologie et géophysique de l'environnement, CNRS*
54, rue Molière, BP 96, 38402 Saint Martin d'Hères, France
lemeur@lgge.obs.ujf-grenoble.fr

[5] *Laboratoire d'Informatique, Systèmes, Traitement de l'Information et de la Connaissance*
LISTIC, CNRS
Polytech'Savoie, 74944 Annecy le Vieux, France
emmanuel.trouve@univ-savoie.fr

ABSTRACT

This paper presents some applications of the Maximum Likelihood (ML) texture tracking on displacement estimation of some alpine and antarctic glaciers surfaces. This method is adapted to the statistical characteristic of the new High Resolution (HR) Polarimetric SAR (PolSAR) data. The ML texture tracking method is firstly reminded and a statistical model of HR PolSAR data is explained. The main part of this paper is focused on the application of this method on glaciers monitoring. Three different glaciers have been chosen to test the algorithm: a cold alpine glacier, a temperate alpine glacier and an outlet antarctic glacier. The accuracy and limits of the method are highlighted in each case and results application is discussed.

Key words: Polarimetric SAR, Texture modeling, ML tracking, glacier.

1. INTRODUCTION

The glaciers are changing due to climate evolution. The consequences of the glaciers reaction are of importance in landscape evolution and may increase some natural risks. The antarctic glaciers are directly representative of the ice cap evolution and some alpine glaciers may represent a threat for some villages in the valleys. SAR imagery and more particularly the new HR SAR sensors represent a powerful tool helpful in monitoring glaciers. Considering the complexity of the glaciers and their high temporal and spatial variability, SAR interferometry may often be faced to some speckle decorrelation. Hence with the new generation of HR PolSAR sensors, the images reach a high level of details and tracking methods have to be focused on an accurate statistical modeling. In reconsidering the usual homogeneous PolSAR clutter model, a new ML tracking method has been derived from the intensity-based method introduced by [1]. Heterogeneous clutter models have therefore recently been studied with PolSAR data through the SIRV processes [2]. This paper is focused on the application of this new ML tracking algorithm previously introduced in [3] on different kind of glaciers

using various polarimetric and non-polarimetric images. The first part is dedicated to the method scheme. Each step is detailed from the texture extraction to the similarity criteria definition. The second part of this paper presents some displacement fields estimations results on RADARSAT-2 (RS2) data acquired on three glaciers.

2. DISPLACEMENT ESTIMATION

The displacement estimation based on the ML tracking method in case of HR PolSAR data may be decomposed in different steps as it is illustrated in Fig. 1. First of all, the texture component τ of these PolSAR data must be extracted through a SIRV process.

2.1. SIRV model

The target vector $\mathbf{k}$ can be decomposed as the product of a square root of a positive random variable τ (representing the texture) with an independent complex Gaussian vector $\mathbf{z}$: $\mathbf{k} = \sqrt{\tau}\,\mathbf{z}$. $\mathbf{z}$ is zero mean and have a covariance matrix $[M] = E\{\mathbf{z}\mathbf{z}^H\}$ (representing the speckle), where the superscript H denotes the complex conjugate transposition and $E\{\cdot\}$ the mathematical expectation.

Here is briefly described the SIRV estimation scheme which is one way to estimate the texture component τ. The principle is an iterative process which estimates both τ and the normalized covariance matrix $[M]$.
For a given covariance matrix $[M]$, the ML estimator of the texture parameter τ for the pixel i ($\hat{\tau}_i$) is given by:

$$\hat{\tau}_i = \frac{\mathbf{k}_i^H [M]^{-1} \mathbf{k}_i}{p},\qquad(1)$$

where p is the dimension of the target scattering vector $\mathbf{k}$ ($p = 3$ in the reciprocal case). For sake of simplicity, in this study the texture component is approximated to a deterministic case. Under this hypothesis, the ML estimator of $[M]$ is solution of:

$$[\hat{M}_{ML}] = f([\hat{M}_{ML}]) = \frac{p}{N} \sum_{i=1}^{N} \frac{\mathbf{k}_i \mathbf{k}_i^H}{\mathbf{k}_i^H [\hat{M}_{ML}]^{-1} \mathbf{k}_i}$$
$$= \frac{p}{N} \sum_{i=1}^{N} \frac{\mathbf{z}_i \mathbf{z}_i^H}{\mathbf{z}_i^H [\hat{M}_{ML}]^{-1} \mathbf{z}_i}.\qquad(2)$$

For more details about the SIRV estimation scheme, reader may refer to [2].

2.2. Texture modeling

After having extracted the texture component τ, a correct statistical description must be found to model τ in order to derive an accurate similarity criterion. Previous studies [4] have exhibited the relevance of the Fisher Probability Density Funvtion (PDF) for modeling τ:

$$p_\tau(\tau) = \mathcal{F}[m, \mathcal{L}, \mathcal{M}] = \frac{\Gamma(\mathcal{L} + \mathcal{M})}{\Gamma(\mathcal{L})\Gamma(\mathcal{M})} \frac{\mathcal{L}}{\mathcal{M}m} \frac{\left(\frac{\mathcal{L}\tau}{\mathcal{M}m}\right)^{\mathcal{L}-1}}{\left(1 + \frac{\mathcal{L}\tau}{\mathcal{M}m}\right)^{\mathcal{L}+\mathcal{M}}}$$
$$(3)$$

where m is a scale parameter, $\mathcal{L}$ and $\mathcal{M}$ are two shape parameters.

2.3. Similarity criterion

The heart of all tracking methods is the same and may be described like in Fig. 2. For each pixel x of the master image, a window τ_x is extracted around it. An other same size window $\tau_y{}^i$ slides on the slave image in a displacement area centered on pixel x. For each position i of $\tau_y{}^i$ a similarity criterion is computed. The coordinates of the maximum of this criterion are the velocity components of x:

$$\overrightarrow{v}_{ML} = \underset{i}{\text{Argmax}}\ p\left(\tau_x | \tau_y^i, \overrightarrow{v}_i\right).\qquad(4)$$
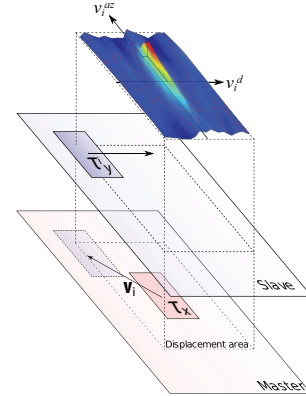

Figure 2. General $\mathbf{v}_{ML}$ searching principle.

In HR PolSAR data context, it may be relevant to define a statistically-based similarity criterion. According to the Fisher PDF texture model, a similarity criterion has been previously derived [3] in both uncorrelated and correlated texture cases. Due to the high temporal variability of the glaciers surface, this paper focuses on the uncorrelated texture case whose similarity criterion is defined as the likelihood function of the ratio PDF of two uncorrelated texture random variables which are Fisher distributed:
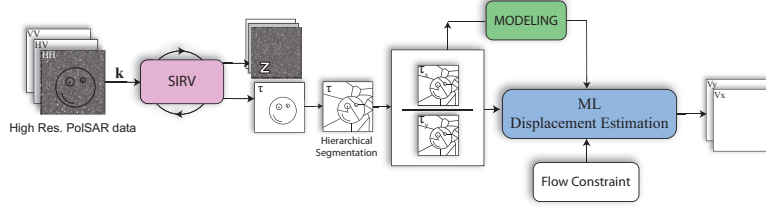
Figure 1. Global scheme of the displacement estimation method.

$$
\mathrm{L}(\overrightarrow{v}_i) = n \ln \left(\frac{B(2\mathcal{L}, 2\mathcal{M})}{[B(\mathcal{L}, \mathcal{M})]^2} \right)
$$

$$
- (\mathcal{M} + 1) \sum_{j=1}^{n} \ln \tau_{x_j} + \mathcal{M} \sum_{j=1}^{n} \ln \tau_{y_j}^i
$$

$$
+ \sum_{j=1}^{n} \ln \left({}_2F_1 \left(\mathcal{L} + \mathcal{M}, 2\mathcal{M}; 2\left(\mathcal{L} + \mathcal{M}\right); 1 - \frac{\tau_{y_j}^i}{\tau_{x_j}} \right) \right).
$$

(5)

where ${}_2F_1(\cdot, \cdot; \cdot; \cdot)$ and $B(\cdot, \cdot)$ are respectively the Gauss hypergeometric function and the Euler Beta function.

2.4. Advanced processing

In referring to Fig. 1, previous subsections have described each colored step, i.e. texture extraction, texture modeling and similarity criterion definition for ML displacement estimation. The current subsection is focused on some additional improvements to refine this method: the hierarchical segmentation of the texture and an additional flow constraint to the similarity criterion are presented.

2.4.1. Hierarchical segmentation

In classical tracking methods, the sliding windows are often rectangle shaped. However in case of a similarity criterion based on statistics, it may be more accurate to draw adaptive windows which will be homogeneous in term of stochastic process. The hierarchical segmentation [5] is a method which divides an image in homogeneous segments under a statistical point of view. A hierarchical segmentation pre-processing step computed on the texture image may enhance the robustness of the ML tracking method: each segment is an adapted sliding window. An example of such segmentation is shown in Fig. 3(b).

2.4.2. Flow constraint

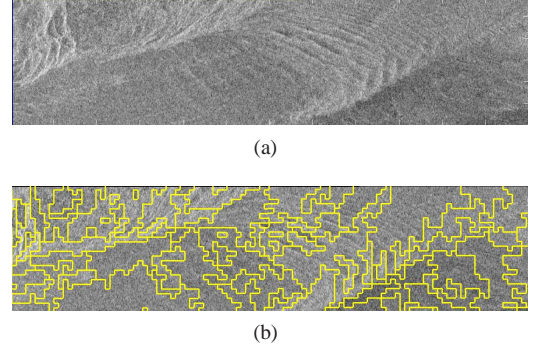A weighted ML-based similarity criterion may be defined in adding a basic *a priori* flow model constraint on the

(a)

(b)

Figure 3. TerraSAR-X (TSX) data 2009-01-06. Argentière glacier. (a) Logarithm of the texture parameter τ estimated using SIRV model. (b) Hierarchical segmentation.

amplitude ρ and the orientation θ of the velocity. According to the Bayes's rule, the problem formulation becomes:

$$
p\left(\tau_y^i, \overrightarrow{v}_i | \tau_x\right) = \frac{p\left(\tau_x | \tau_y^i, \overrightarrow{v}_i\right) p\left(\tau_y^i | \overrightarrow{v}_i\right) p\left(\overrightarrow{v}_i\right)}{p\left(\tau_x\right)}
$$

(6)

Let ρ_i and θ_i be the independent polar coordinates of the displacement vector $\overrightarrow{v}_i$. In (6), the prior term $p\left(\overrightarrow{v}_i\right)$ can be rewritten as:

$$
p\left(\overrightarrow{v}_i\right) = p_\rho\left(\rho_i\right) p_\theta\left(\theta_i\right)
$$

(7)

They are linked with the distance v_i^d and azimuth v_i^{az} component by $\rho_i = \sqrt{v_i^{d^2} + v_i^{az^2}}$ and $\theta_i = \mathrm{atan}(v_i^{az}/v_i^d)$.

In this study $p_\rho\left(\rho_i\right)$ is uniform and $p_\theta\left(\theta_i\right)$ is a circular analog of the normal distribution centered on the maximum downhill slope angle.

3. RESULTS

The ML tracking method has been tested on the displacement estimation of three different glaciers. Two of them are alpine glaciers and one is an outlet antarctic glacier. A picture of them is shown in Fig. 4.
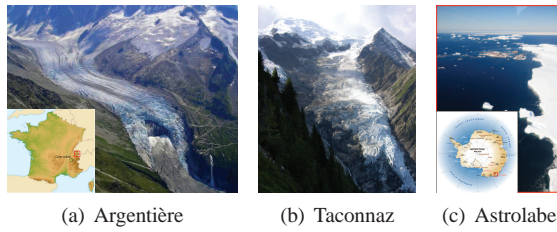
(a) Argentière   (b) Taconnaz   (c) Astrolabe

Figure 4. Test sites: (a) (b) alpine and (c) antarctic glaciers.

3.1. Alpine glaciers
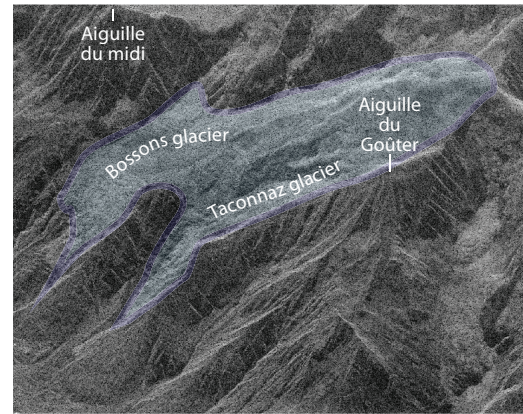
3.1.1. A cold glacier: the Taconnaz glacier

The Taconnaz glacier which is located in the Mont Blanc massif in french Alps is a cold alpine glacier which means that its internal temperature is always below 0°C. Due to the bedrock topography, a high ice cliff develops over most of the glacier width separating the glacier into an upper accumulation area and a lower ice tongue [6]. The large ice falls breaking off the glacier at 3300 m ASL are responsible for large avalanches of snow and ice which can cause serious damage in the valley. Because of its location above the Chamonix town, it is considered as a "at-risk" glacier.

Fig. 3.1.1 shows some displacement estimations on the surface of the Taconnaz glacier without any advanced processing like adaptive sliding window or flow constraint. The orientation map is very relevant with the reality as it is oriented through the downhill slope. The velocity amplitude is in Line Of Sight (LOS) and has to be projected to the ground, however the slope is steep that is why the projected values and the LOS values may be of the same order of magnitude. The two peaks of velocity which are about one meter a day, are located on the serac fall. Such a monitoring method provides a fine temporal analysis.

3.1.2. A temperate glacier: the Argentière glacier

The Argentière glacier is a temperate alpine glacier and is located also in the Mont Blanc massif. This glacier is well monitored for years and since 2006 some corner reflectors are set on its surface. In contrary of the Taconnaz glacier, its relief is more regular. Its upper part is located at about 3000m ASL and it flows down to a unique serac fall at about 2000m ASL.

In the case of the Argentière glacier, a large part of its surface is quite homogeneous and it is very hard to track any displacement. However when using an adaptive sliding window associated with a flow constraint, the similarity criterion may retrieve some relevance. Fig. 6(d) illustrates such results on a segmented images pair: the

(a) Master image. RS2 29-01-2009
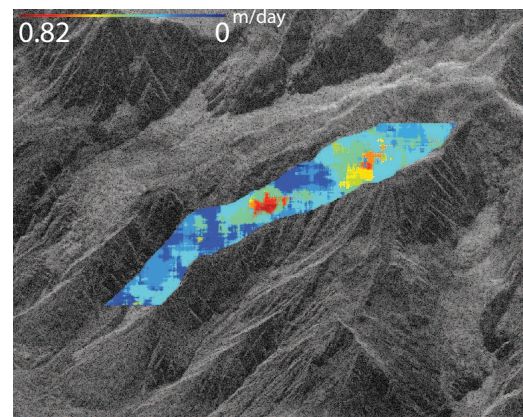
(b) Displacement field in LOS
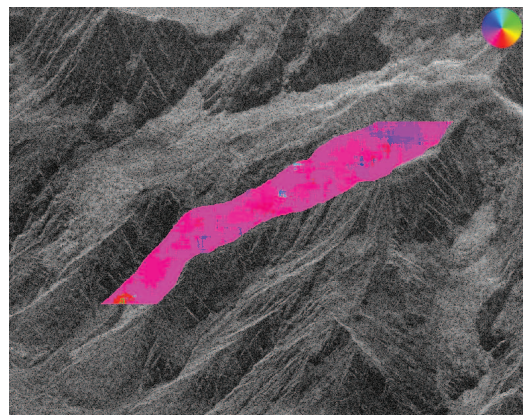
(c) Orientation map

Figure 5. Displacement estimation on the surface of the Taconnaz glacier

orientation map is very accurate compared to the real orientation map computed from a Digital Elevation Model (DEM). Moreover the velocity amplitude is accurate because the displacement is null on the glacier banks whereas a velocity peak is observable on the crevasses area which is effectively the steepest slope area of this crop.
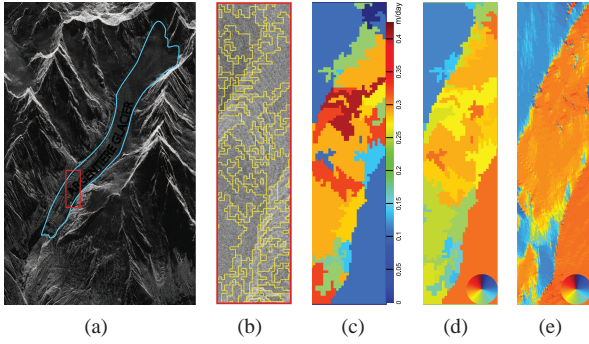
Figure 6. Dual-pol TSX data, 2009-01-06 / 2009-02-08. Displacement estimation over a crevasses area on the Argentière glacier using segmented texture images.(a) Master image. TSX 2009-01-06. (b) Master image segmented. (c) Displacement field in LOS. (d) Estimated orientation map with flow constraint. (e) Real orientation map.

3.2. An outlet Antarctic glacier: the Astrolabe glacier

Big ice caps have a high environmental potential in particularly on the sea level. For instance, the Antarctic ice cap is equivalent to a volume of 70m of sea level. Outlet antarctic glaciers play a role of ice cap flow regulator into the sea. They are like the tap of the ice cap. The astrolabe glacier is one of the rare monitored outlet Antarctic glaciers on the east coast. It is located near the french Dumont Durville scientific station which makes the logistics easier.
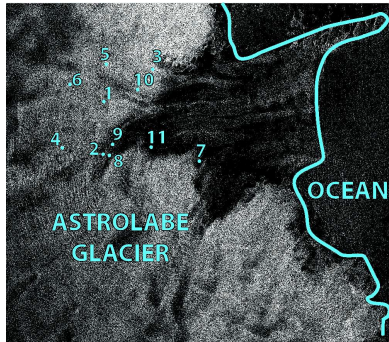

Figure 7. Master image of the Astrolabe glacier with GPS points location.

Some GPS data are available on this glacier. After having projected some displacement estimations on the ground, some comparisons have been made between the estimated velocity and the GPS values. These preliminary results are shown in Fig. 9. In considering the spatial and temporal variability of the velocity due to the accidental relief of the Astrolabe glacier tongue and due to some surges effects, these preliminary comparisons have to be taken with caution. The GPS data and the RS2 acquisitions are indeed not synchronized and the geolocalization of the GPS points on the SAR images are furthermore approximate.

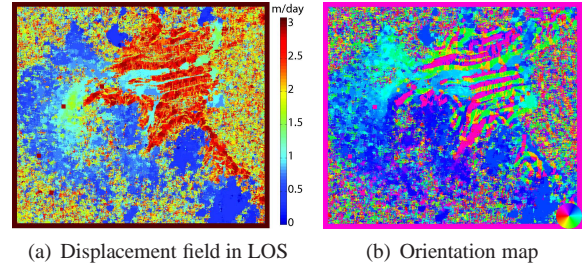(a) Displacement field in LOS   (b) Orientation map

Figure 8. Displacement estimation on the surface of the Astrolabe glacier.
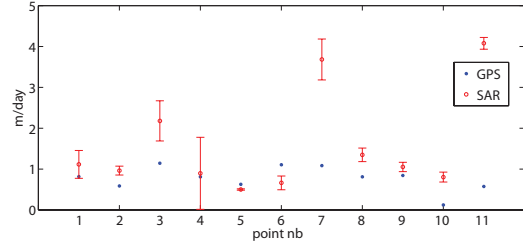

Figure 9. Comparison of displacement estimation with GPS data.

In the contrary of the previous glaciers, this displacement estimation has been performed from single polarimetric RS2 data. Hence, the velocity field shown in Fig. 8(a) has been computed with the classical ML texture tracking method introduced in [1]. The estimated displacement shown in Fig. 8(a) underline various behavior of the algorithm: in the case of no-textured areas like the ice cap or high temporally variable areas like ocean, the results are very noisy. But in the other cases, the displacement is quite relevant and an acceleration may be observed from the catchment of the glacier on the left to the glacier tongue on the right. Moreover, the orientation map is also accurate as the velocity field converges to the glacier tongue direction (Fig. 8(b)).

4. CONCLUSION

Through the volumetric characteristics of the glaciers surface, polarimetry offers a amount of information which may improve tracking methods and texture estimation. In this study, the SIRV process uses the polarimetric channels to decorrelate the texture from the speckle component.

This paper has presented some applications of the ML texture tracking method on polarimetric and non polarimetric RS2 data for surface displacement estimation on the surface of glaciers. Three glaciers have been selected: one alpine cold glacier (the Taconnaz glacier), one temperate alpine glacier (the Argentière glacier) and one outlet antarctic glacier (the Astrolabe glacier). More accidental is the glacier, more textured is the SAR image. It yields that the robuster is the method. However in case of homogeneous glacier surface, some advanced processing

should be added to retrieve such robustness as it has been shown in case of the Argentière glacier.

Future works will be focused on the merging of various HR PolSAR sensors to generalize this method to a multi-frequency as well as multi-resolution method.

ACKNOWLEDGEMENT

REFERENCES

1. E. Erten, A. Reigber, O. Hellwich, and P. Prats. Glacier Velocity Monitoring by Maximum Likelihood Texture Tracking. *IEEE Transactions on Geoscience and Remote Sensing*, 47(2):394–405, 2009.

2. G. Vasile, J.-P. Ovarlez, F. Pascal, and C. Tison. Coherency Matrix Estimation of Heterogeneous Clutter in High Resolution Polarimetric SAR Images. *IEEE Transactions on Geoscience and Remote Sensing*, 48(4):1809 – 1826, 2010.

3. O. Harant, L. Bombrun, G. Vasile, L. Ferro-Famil, and M. Gay. Displacement estimation by maximum likelihood texture tracking. *Journal of Selected Topics in Signal Processing, JSTSP '11*, to appear, 2011.

4. L. Bombrun and J.-M. Beaulieu. Fisher Distribution for Texture Modeling of Polarimetric SAR Data. *IEEE Geoscience and Remote Sensing Letters*, 5(3), July 2008.

5. L. Bombrun and J.-M. Beaulieu. Segmentation of Polarimetric SAR Data Based on the Fisher Distribution for Texture Modeling. In *Geoscience and Remote Sensing, IGARSS '08, Boston, USA*, 2008.

6. E. Le Meur and C. Vincent. Monitoring of the Taconnaz ice fall (French Alps) using measurements of mass balance, surface velocities and ice cliff position. *Cold Regions Science and Technology*, 46(1):1–11, 2006.